Extending anticipation horizon of chaos synchronization schemes with time-delay coupling

By Kestutis Pyragas[1,2] and Tatjana Pyragienė[1]

[1]*Semiconductor Physics Institute, 11 A. Goštauto, LT-01108 Vilnius, Lithuania*
[2]*Faculty of Physics, Vilnius University, LT-10222 Vilnius, Lithuania*

We analyze anticipating synchronization in chaotic systems with time-delay coupling. Two algorithms for extending the prediction horizon are considered. One of them is based on design of a suitable coupling matrix compensating the phase-lag in the time-delay feedback term of the slave system. The second algorithm extends the first by incorporating in the coupling law information from many previous states of the master and slave systems. We demonstrate the efficiency of both algorithms with the simple dynamical model of coupled unstable spirals as well as with the coupled Rössler systems. The maximum prediction time attained for the Rössler system is equal to the characteristic period of chaotic oscillations.

Keywords: anticipating synchronization of chaos, time-delay feedback, coupling design

1. Introduction

Synchronization of oscillations has been known to scientists since the historical discovery of this phenomenon by Huygens in pendulum clocks. Later on, synchronization was observed and shown to play an important role in a large variety of systems in physics, chemistry, and biology [Pikovsky *et al.* (2001), Boccaletti *et al.* (2002)]. Original notion and classical theory of synchronization implies periodicity of oscillators. The discovery of chaotic oscillators has originated a new subfield in nonlinear dynamics referred to as synchronization of chaos. A generic feature of nonlinear systems exhibiting chaotic motions is the extreme sensitivity to initial conditions. This feature, known as the butterfly effect, would seem to defy synchronization among dynamical variables in coupled chaotic systems. Nonetheless, several different regimes of chaos synchronization have been discovered and investigated over the past two decades.

Afraimovich (1986) and Pecora & Carrol (1990) introduced the notion of identical chaos synchronization. Here the coupled chaotic systems are identical and synchronization appears as a coincidence of corresponding variables of coupled systems $\mathbf{r}_2(t) = \mathbf{r}_1(t)$ as t approaches infinity. The identical chaos synchronization in time-delay systems was considered by Pyragas (1998). Rulkov *et al.* (1995) showed that synchronization may appear in unidirectionally coupled non-identical chaotic systems as a functional relationship $\mathbf{r}_2(t) = \mathbf{F}[\mathbf{r}_1(t)]$ between the variables of the drive (master) $\mathbf{r}_1$ and response (slave) $\mathbf{r}_2$ systems. This type of synchronization is called the generalized synchronization. Generalized synchronization can also appear

in weakly coupled identical chaotic systems and usually precedes the identical synchronization [Pyragas (1996)]. A particular case of the generalized synchronization is the projective synchronization, when there exists a scale factor in the amplitude of the master's state variable and that of the slave's, i.e., $\mathbf{r}_2(t) = \alpha \mathbf{r}_1(t)$ [Mainieri *et al.* (1999)]. Rosenblum *et al.* (1996) detected phase synchronization, which means the difference between the phase of the master's state and that of the slave's, is constant during interaction, whereas their amplitudes remain chaotic and uncorrelated, i.e., $n\varphi_1 - m\varphi_2 = const$ (n and m are integers). Another type of chaos synchronization introduced by Rosenblum *et al.* (1997) is the lag synchronization, when the state of slave is retarded with the time length of τ compared to that of master, i.e., $\mathbf{r}_2(t) = \mathbf{r}_1(t-\tau)$.

More recently Voss (2000) discovered so-called anticipating synchronization of chaos, which is most counterintuitive among the types of synchronization listed above. Here unidirectionally coupled systems synchronize in such a way that the slave system predicts the behavior of the master system, i.e., $\mathbf{r}_2(t) = \mathbf{r}_1(t+\tau)$. Voss considered two coupling schemes. The first scheme implies the presence of an internal delay in the master system and the coupling is introduced by complete replacement of the variables:

$$\dot{\mathbf{r}}_1(t) = -\beta \mathbf{r}_1(t) + \mathbf{f}\left(\mathbf{r}_1(t-\tau)\right) \tag{1.1a}$$

$$\dot{\mathbf{r}}_2(t) = -\beta \mathbf{r}_2(t) + \mathbf{f}(\mathbf{r}_1(t)). \tag{1.1b}$$

Here $\mathbf{r}_1(t)$ and $\mathbf{r}_2(t)$ are the dynamic vector variables of the master and slave system, respectively, $\mathbf{f}$ is a nonlinear vector function, τ is a delay time, and β is a scalar parameter. It is easy to see that the anticipatory synchronization manifold $\mathbf{r}_2(t) = \mathbf{r}_1(t+\tau)$ is a solution of Eqs. (1.1). The stability of this manifold is defined by equation for the difference $\mathbf{\Delta}(t) = \mathbf{r}_1(t+\tau) - \mathbf{r}_2(t)$, which is simply derived from Eqs. (1.1)

$$\dot{\mathbf{\Delta}}(t) = -\beta \mathbf{\Delta}(t). \tag{1.2}$$

For $\beta > 0$ the anticipatory synchronization manifold is globally stable. Thus the slave anticipates by an amount τ the output of the master.

In the second scheme proposed by Voss, the master system does not possess an internal delay, however, the delay is introduced in the coupling term of the slave system:

$$\dot{\mathbf{r}}_1(t) = \mathbf{f}(\mathbf{r}_1(t)) \tag{1.3a}$$

$$\dot{\mathbf{r}}_2(t) = \mathbf{f}(\mathbf{r}_2(t)) + k\mathbf{K}[\mathbf{r}_1(t) - \mathbf{r}_2(t-\tau)]. \tag{1.3b}$$

Here k is a scalar parameter defining the coupling strength and $\mathbf{K}$ is a coupling matrix. Again, one can check that the anticipatory synchronization manifold $\mathbf{r}_2(t) = \mathbf{r}_1(t+\tau)$ is a solution of Eqs. (1.3). However, the proof of stability of this manifold is more complicated task as for the first scheme. While in the scheme of complete replacement the anticipation time τ coincides with the internal delay time of the master system and can be arbitrarily large, the delay coupling scheme requires some constraints on the anticipation time τ and coupling $\mathbf{K}$ for the synchronization solution to be stable. Despite this fact, the delay coupling scheme is more interesting and promising for applications, since it does not require the presence of delay in the master system and the anticipation time τ can be varied without altering the master's dynamics.

Anticipating synchronization of chaos has been studied numerically for a variety of systems by Masoller *et al.* (2001), Calvo *et al.* (2004), Kostur *et al.* (2005) and justified experimentally in electronic circuits by Voss *et al.* (2002) and chaotic semiconductor lasers by Sivaprakasam *et al.* (2001), and Tang *et al.* (2003). It has been also observed in excitable systems driven by random forcing [Ciszak *et al.* (2003), Ciszak *et al.* (2004)].

Implementation of anticipating synchronization as a strategy for real-time forecasting of a given dynamics requires the design of coupling schemes with a possibly large anticipation time. The analysis performed by Voss (2000) shows that the scheme (1.3) with a diagonal matrix $\mathbf{K}$ is ineffective. Its maximum stably anticipation time is much shorter than the characteristic time scales of the system‘s dynamics. In order to enlarge the prediction time Voss (2001) proposed to extend Eq. (1.3b) with a chain of N unidirectionally coupled slave systems:

$$\dot{\mathbf{r}}_i(t) = \mathbf{f}(\mathbf{r}_i(t)) + k\mathbf{K}[\mathbf{r}_{i-1}(t) - \mathbf{r}_i(t-\tau)], \quad i = 2, \ldots, N+1. \tag{1.4}$$

Formally, the prediction time of this scheme is N times larger as compared to the scheme (1.3b). However, Mendoza *et al.* (2004) showed that the chain (1.4) is unstable to propagating perturbations and this convectivelike instability limits the number of slaves in the chain which can operate in a stable regime.

In our recent publication [Pyragas & Pyragienė (2008)], we addressed the question of whether the prediction time can be considerably enlarged with the single slave system (1.3b) via a suitable choice of the coupling matrix $\mathbf{K}$. For typical low-dimensional chaotic systems we gave a positive answer. We proposed an algorithm of design $\mathbf{K}$ based on a phase-lag compensating coupling (PLCC) and showed that the prediction time can be enlarged several times in comparison to the diagonal coupling usually used in the literature. Here we further develop this idea by introducing an extended PLCC (EPLCC) and show that the prediction horizon can be prolonged to the characteristic period of chaotic oscillations.

2. Phase-lag compensating coupling

We demonstrate a heuristic idea of PLCC algorithm with the Rössler (1976) system, which is given by a three-dimensional vector variable $\mathbf{r} = [x, y, z]$ and vector field

$$\mathbf{f}(\mathbf{r}) = [-y - z, x + ay, b + z(x - c)]. \tag{2.1}$$

In the following we set $a = 0.15$, $b = 0.2$, $c = 10$ and suppose that both $\mathbf{r}$ and $\mathbf{f}$ are the vectors columns. The phase portrait of the Rössler system for the given values of the parameters is shown in Fig. 1. Although the Rössler system has two fixed points, the strange attractor is originated from one of them $\mathbf{r}_0 = [(c - s)/2, (s - c)/2a, (c - s)/2a]$ located close to the origin, where $s = (c^2 - 4ab)^{1/2}$. The fixed point is a saddle-focus with an unstable 2D manifold (an unstable spiral) almost coinciding with the (x, y) plane and a stable 1D manifold almost coinciding with the z axis. The phase point of the system spends most time in the (x, y) plane moving along the unstable spiral according to approximate equations $\dot{x} = -y$, $\dot{y} = x + ay$. Whenever x approaches a value $x \approx c$, the z variable comes into play. The phase point leaves for a short time the (x, y) plane and then returns to the origin via a stable z-axis manifold.

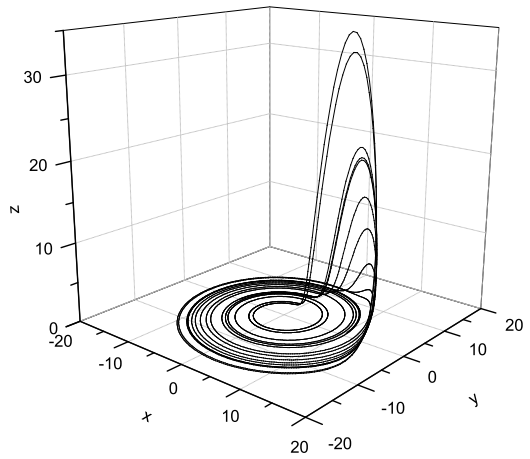

Figure 1. Phase portrait of the Rössler system for $a = 0.15$, $b = 0.2$ and $c = 10$.

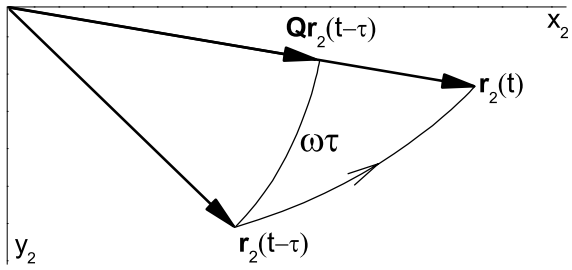

Figure 2. Phase-lag compensation of the time-delayed vector $\mathbf{r}_2(t-\tau)$.

Taking into account such a topology of the strange attractor we choose the coupling matrix as $\mathbf{K} = \mathbf{Q}$, where

$$\mathbf{Q} = \begin{pmatrix} \cos\alpha & -\sin\alpha & 0 \\ \sin\alpha & \cos\alpha & 0 \\ 0 & 0 & 0 \end{pmatrix} \tag{2.2}$$

is a 3×3 matrix that projects the vector field onto the unstable (x, y) plane and rotates this projection by the angle $\alpha = \omega\tau$. Here ω is a frequency of the unstable spiral, which for the Rössler system is ≈ 1. The main advantage of such a choice consists in phase-lag compensation of the time-delay feedback term in Eq. (1.3b). When the system moves along the unstable spiral in the (x, y) plane, the vector $\mathbf{Q}\mathbf{r}_2(t-\tau)$ is in-phase with the vector $\mathbf{r}_2(t)$ [cf. Fig. 2], and thus the term $\mathbf{K}\mathbf{r}_2(t-\tau)$ provides a correct negative feedback. We refer to this coupling law as a phase-lag compensating coupling (PLCC). In Figs. 3 (a) and (b) we compare the effect of PLCC with the usual diagonal coupling, when $\mathbf{K} = \mathrm{diag}[1, 1, 1]$. The time of reliable prediction for the PLCC is $\tau \approx 3.8$. It exceeds 4 times the maximum prediction time for the diagonal coupling. The characteristic period of chaotic oscillations for the Rössler system is $T \approx 6.3$. Thus the PLCC algorithm allows us to make prediction for more than a half of this period.

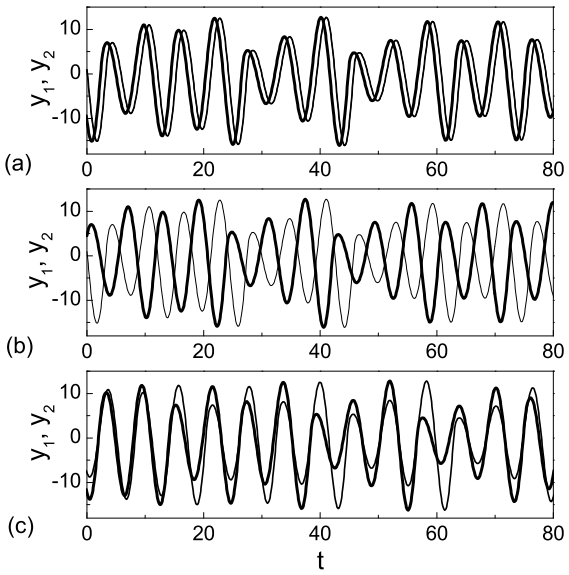

Figure 3. Time series $y_1(t)$ of the master (thin line) and $y_2(t)$ of the slave (bold line) Rössler systems. (a) The diagonal coupling with $\mathbf{K} = \mathrm{diag}[1, 1, 1]$, $k = 0.36$ and $\tau = 0.9$. (b) The PLCC with $\mathbf{K} = \mathbf{Q}$, $k = 0.18$, $\omega = 0.997$, and $\tau = 3.6$. (c) The EPLCC with $\mathbf{K} = \mathbf{EQE}^{-1}$, $k = 0.18$, $\omega = 0.997$, $R = -0.46$ and $\tau = 6.3$. In all cases the coupling parameters are optimized in such a way as to attain the maximum stably anticipation time.

We stress, that the PLCC enables forecasting of the *global* dynamics of the system, although the coupling matrix (2.2) takes into account only the *local* properties of the phase space. Indeed, the phase-lag compensation via rotation of the vector field is strongly valid only in the vicinity of the fixed point. It is notable that a similar rotation feedback gain has been recently used by Fiedler *et al.* (2007) in a problem of the delayed feedback control [Pyragas (1992)] to overcome the so-called odd number limitation.

The success of the PLCC algorithm can be explained by a simple analytical model. The instability of the Rössler attractor is defined by the unstable spiral lying in the (x, y) plane, where the phase point of the system spends most time. Thus one can expect that the main properties of anticipating synchronization of the Rössler systems can be derived from local motion on the unstable spirals, i.e., by considering the simplified problem of anticipating synchronization of the mere spirals. Specifically, assume that dynamical system under consideration is described by two linear equations $\dot{x} = \gamma x - \omega y$, $\dot{y} = \omega x + \gamma y$ that define an unstable spiral with the positive increment γ and frequency ω. For the complex variable $Z = x + iy$, this system can be presented by a single equation $\dot{Z} = (\gamma + i\omega)Z$. Then equations for anticipating synchronization of two spirals take the form

$$\dot{Z}_1(t) = (\gamma + i\omega)Z_1(t) \tag{2.3a}$$

$$\dot{Z}_2(t) = (\gamma + i\omega)Z_2(t) + k\mathrm{e}^{i\alpha}[Z_1(t) - Z_2(t - \tau)], \tag{2.3b}$$

where $k\mathrm{e}^{i\alpha}$ is a complex coupling coefficient. By a suitable choice of the phase α we can model both the PLCC ($\alpha = \omega\tau$) and diagonal coupling ($\alpha = 0$). The

solution of the master system is $Z_1(t) = Z_0 \mathrm{e}^{(\gamma+i\omega)t}$ and the deviation $\delta Z_2(t) = Z_2(t) - Z_0 \mathrm{e}^{(\gamma+i\omega)(t+\tau)}$ from the anticipated state satisfies $\delta \dot{Z}_2(t) = (\gamma + i\omega)\delta Z_2(t) - k\mathrm{e}^{i\alpha}\delta Z_2(t-\tau)$. Substituting $\delta Z_2(t) = C\mathrm{e}^{(\lambda+i\omega)t}$ we obtain the characteristic equation

$$\lambda = \gamma - k\mathrm{e}^{i(\alpha-\omega\tau)}\mathrm{e}^{-\lambda\tau} \tag{2.4}$$

that defines the eigenvalues λ of the synchronized state in a rotating frame with the frequency ω; the real parts of λ represent the transversal Lyapunov exponents of the anticipation manifold. For PLCC, $\alpha = \omega\tau$ and solution of Eq. (2.4) is

$$\lambda = \gamma + W(-\tau k\mathrm{e}^{-\gamma\tau})/\tau, \tag{2.5}$$

where W(z) is the Lambert W function, satisfying by definition $W(z)\mathrm{e}^{W(z)} = z$ [Corless *et al.* (1996)]. The dependence of the leading transversal Lyapunov exponent $\mathrm{Re}\lambda$ on the coupling strength k is shown in Fig. 5 (a); it is determined by the principal branch of the Lambert function. The synchronized state is stable in some interval of the coupling strength $k_1 < k < k_2$, where $\mathrm{Re}\lambda(k) < 0$. The lower bound of stability is determined by the spiral's increment, $k_1 = \gamma$ and is independent of τ. The dependence of the upper bound on τ, $k_2 = k_2(\tau)$ is defined by the parametric equation presented in the caption of Fig. 4. The leading transversal Lyapunov exponent reaches the minimal value $\mathrm{Re}\lambda(k_0) = \gamma - 1/\tau$ at $k_0 = \mathrm{e}^{\gamma\tau-1}/\tau$. Thus the necessary condition for stability of the synchronized state is $\mathrm{Re}\lambda(k_0) < 0$ or

$$\tau < \tau_H = 1/\gamma, \tag{2.6}$$

where τ_H is the prediction horizon. As expected from a general theory, the limit for prediction horizon is determined by the inverse of the largest Lyapunov exponent of the system, which for the spiral is $1/\gamma$. In figure 4, we compare stability regions in the (τ, k) plane for the PLCC ($\alpha = \omega\tau$) and diagonal coupling ($\alpha = 0$). We see that the region of PLCC is considerably larger than that of the diagonal coupling. Note that these regions are in approximate quantitative agreement with the corresponding regions of the Rössler system [cf. Pyragas & Pyragienė (2008)]. Thus the characteristic parameters of anticipating chaotic synchronization can be estimated analytically from the simple linear Eqs. (2.3) that model local dynamics of the chaotic system close to the fixed point.

The PLCC algorithm can be generalized for any Rössler-type chaotic system. Suppose that a strange attractor of a three-dimensional dynamical system

$$\dot{\mathbf{r}} = \mathbf{f}(\mathbf{r}) \tag{2.7}$$

is originated from a saddle-focus fixed point $\mathbf{r}_0$ such that $\mathbf{f}(\mathbf{r}_0) = 0$. Generally, the unstable and stable manifolds of the fixed point may have arbitrary orientations in the phase space. To design the coupling for this general case we first shift coordinates to the fixed point and rewrite the governing equation in the form

$$\dot{\mathbf{R}} = \mathbf{J}\mathbf{R} + \mathbf{N}(\mathbf{R}), \tag{2.8}$$

where $\mathbf{J} = \partial\mathbf{f}/\partial\mathbf{r}|_{\mathbf{r}=\mathbf{r}_0}$ is the Jacobian matrix, $\mathbf{N}(\mathbf{R}) = \mathbf{f}(\mathbf{r}_0+\mathbf{R}) - \mathbf{J}\mathbf{R}$ is a nonlinear function and $\mathbf{R} = \mathbf{r} - \mathbf{r}_0$. Then Eq. (1.3b) for the slave system can be written as

$$\dot{\mathbf{R}}_2 = \mathbf{J}\mathbf{R}_2 + \mathbf{N}(\mathbf{R}_2) + k\mathbf{K}[\mathbf{R}_1 - \mathbf{R}_2(t-\tau)]. \tag{2.9}$$

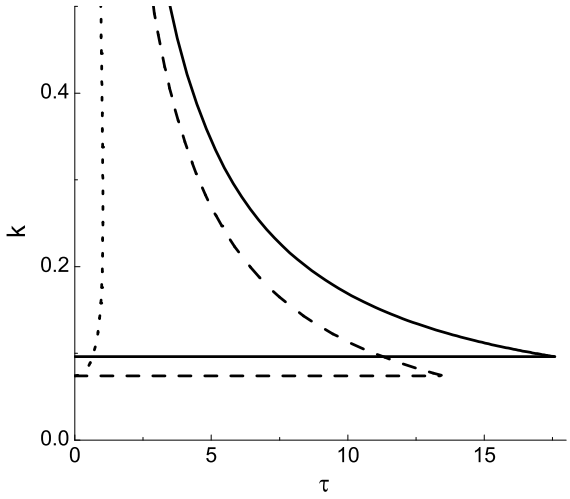

Figure 4. $\tau - k$ stability diagrams for coupled spirals with the parameters $\omega = 0.997$ and $\gamma = 0.074$ the same as the eigenvalues of the fixed point of the Rössler system. The dotted line bounds the region of stability for the diagonal coupling coupling ($\alpha = 0$). It is defined by parametrical equations $\tau(\Omega) = \arctan((\Omega - \omega)/\gamma)/\Omega$, $k(\Omega) = \gamma/\cos(\Omega\tau)$ with the parameter $\Omega \in [\omega, \infty]$. The boundaries of stability for PLCC are depicted by dashed lines. The lower bound is determined by $k_1 = \gamma$. The upper bound is defined parametrically, $k_2(\Omega) = (\gamma^2 + \Omega^2)^{1/2}$, $\tau(\Omega) = \arctan(\Omega/\gamma)/\Omega$, where $\Omega \in [0, \infty]$. The solid lines confine the region of stability of the synchronization manifold for EPLCC at $R = -0.3$. The lower bound is determined by $k_1 = (1 - R)\gamma$. The upper bound is defined by parametrical equations (3.7).

According to our assumptions, the Jacobian $\mathbf{J}$ has a pair of complex conjugate eigenvalues $\lambda_{1,2} = \gamma \pm i\omega$ with $\gamma > 0$, corresponding to 2D unstable spiral manifold, and a real negative eigenvalue λ_3, representing the stable 1D manifold. By a suitable change of variables, the Jacobian $\mathbf{J}$ can be transformed to Jordan normal form, that is

$$\mathbf{E}^{-1}\mathbf{J}\mathbf{E} = \begin{pmatrix} \gamma & -\omega & 0 \\ \omega & \gamma & 0 \\ 0 & 0 & \lambda_3 \end{pmatrix}, \tag{2.10}$$

where $\mathbf{E}$ is the matrix of eigenvectors of $\mathbf{J}$. This transformation orients the unstable 2D manifold towards the (x, y) plane and the stable manifold towards the z axis. After such a transformation we can apply the above theoretical arguments and use the coupling law $\mathbf{K} = \mathbf{Q}$. This means that in the original (non-transformed) variables the coupling matrix has to be constructed as

$$\mathbf{K} = \mathbf{E}\mathbf{Q}\mathbf{E}^{-1}. \tag{2.11}$$

Equation (2.11) gives a general algorithm of coupling design for typical chaotic systems. Application of the general coupling law (2.11) to the Rössler system does not advance significantly the forecasting algorithm in comparison to the above considered heuristic approach. This is because the Jacobian of the Rössler system is close to Jordan normal form and the matrix $\mathbf{E}\mathbf{Q}\mathbf{E}^{-1}$ does not differ significantly from the matrix $\mathbf{Q}$. The coupling law (2.11) works well not only for mono-scroll

chaotic attractors, but it also extends considerably the prediction time of double-scroll chaotic systems, like the Chua circuit or the Lorenz system [cf. Pyragas & Pyragienė (2008)].

3. Extended phase-lag compensating coupling

To further improve the PLCC algorithm we employ an idea from delayed feedback control (DFC) theory [cf. Pyragas (2006)]. The aim of this theory is the stabilization of unstable periodic orbits embedded in chaotic attractors. In the original DFC algorithm [cf. Pyragas (1992)], the coupling law is analogous to that of the anticipating synchronization. Gauthier *et al.* (1994) proposed an extension of the original DFC algorithm, which incorporates in the feedback loop information from many previous states of the system in the form closely related to the amplitude of light reflected from Fabry-Perot interferometer. This modification, known as an extended DFC (EDFC), improves the algorithm considerably. The EDFC makes possible the stabilization of high-periodic orbits with large positive Lyapunov exponents [cf. Pyragas (1995)].

Here we use the idea of extended time-delay feedback in order to improve the performance of the PLCC algorithm. We refer to this modification as an extended PLCC (EPLCC). Whereas the PLCC utilizes the single difference between the current state of the master system and time-delayed state of the response system, the EPLCC extends this perturbation to an infinite series of corresponding differences time-delayed by integer multiples of τ. We first demonstrate the idea for two coupled unstable spirals:

$$\dot{Z}_1(t) = (\gamma + i\omega)Z_1(t), \tag{3.1a}$$

$$\dot{Z}_2(t) = (\gamma + i\omega)Z_2(t) + kS(t). \tag{3.1b}$$

The EPLCC perturbation $S(t)$ is governed by

$$S(t) = \mathrm{e}^{i\alpha}\left[Z_1(t) - Z_2(t-\tau)\right] \tag{3.2a}$$

$$+ \sum_{n=1}^{\infty} R^n\ \mathrm{e}^{i(n+1)\alpha}\left[Z_1(t-n\tau) - Z_2(t-(n+1)\tau)\right], \tag{3.2b}$$

where R is a memory parameter that regulates the weight of time-delayed information. We require $-1 < R < 1$ in order to guarantee the convergence of the infinite sum. The case when $R = 0$ corresponds to phase-lag compensating coupling (PLCC) considered in the previous section [cf. Eq. (2.3b)]. Note that $S(t)$ vanishes for any value of R when the system moves along the synchronization manifold since the equality $Z_1(t-n\tau) = Z_2(t-(n+1)\tau)$ holds on the manifold for all n. The phase-lag of each term in the sum is compensated by the multiplier $\mathrm{e}^{i(n+1)\alpha}$ and the amplitude is weighted by the multiplier R^n such that contribution of terms exponentially decreases with the increase of time-delay.

At the first look the perturbation (3.2) seems to be very complex. Fortunately, the infinite sum can be rewritten in an equivalent, recursive form

$$S(t) = \mathrm{e}^{i\alpha}\left[Z_1(t) - Z_2(t-\tau) + RS(t-\tau)\right] \tag{3.3}$$

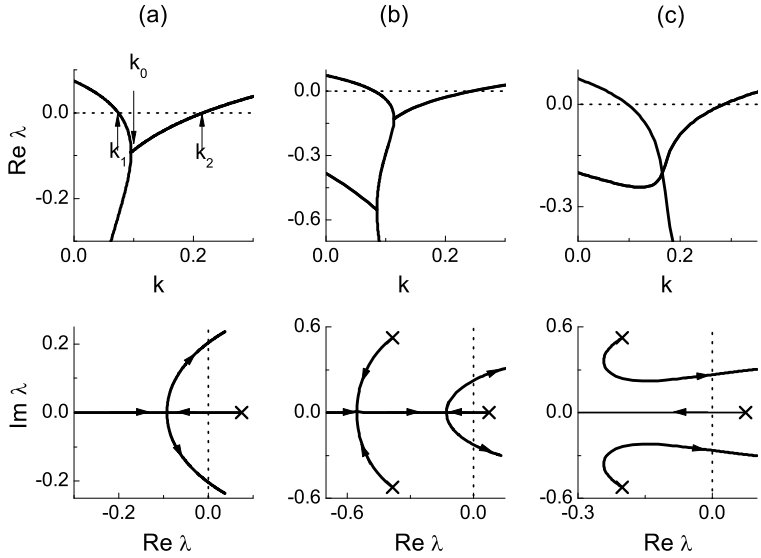

Figure 5. Leading eigenvalues of characteristic equation (3.6) for parameters $\gamma = 0.074$ and $\omega = 0.997$ the same as the eigenvalues of the fixed point of the Rössler system. The delay time is $\tau = 6$. In upper row the dependence of leading transversal Lyapunov exponents on the coupling strength k are shown. In bottom row the root loci diagrams are presented. The crosses denote the location of roots at $k = 0$ and the arrows show the direction of their evolution when k is increased. Different columns correspond to different values of the memory parameter R: (a) simple PLCC, i.e. $R = 0$; (b) EPLCC with $R = -0.1$; (c) EPLCC with $R = -0.3$.

and implemented experimentally with the single delay line [cf. Gauthier *et al.* (1994)]. Now the stability of the synchronized state is defined by variational equations

$$\dot{\Delta}(t) = (\gamma + i\omega)\Delta - kS(t-\tau) \tag{3.4a}$$

$$S(t) = \mathrm{e}^{i\alpha}[\Delta(t) + RS(t-\tau)], \tag{3.4b}$$

where $\Delta(t) = Z_1(t) - Z_2(t-\tau)$ describes the deviation from the synchronization manifold. This leads to the characteristic equation

$$(\lambda - \gamma)(\mathrm{e}^{-i(\alpha-\omega\tau)+\lambda\tau} - R) + k = 0. \tag{3.5}$$

For $R = 0$ it coincides with Eq. (2.4) analyzed in the previous section. Here as well as in the previous section we set $\alpha = \omega\tau$ and analyze the simplified version of Eq. (3.5)

$$(\lambda - \gamma)(\mathrm{e}^{\lambda\tau} - R) + k = 0. \tag{3.6}$$

Unfortunately, the solution of Eq. (3.6) for $R \neq 0$ cannot be expressed through the Lambert function. Numerical solutions of this equation for different values of R are presented in Fig. 5. We see that the negative values of R improve the stability properties of the synchronization manifold.

Although an analytical solution of Eq. (3.6) is not available the boundaries of stability can be obtained analytically. The lower bound of stability $k_1 = \gamma(1 - R)$

is deduced from Eq. (3.6) by substituting $\lambda = 0$. The upper bound of stability k_2 is defined by a Hopf bifurcation. Substituting in Eq. (3.6) $\lambda = i\Omega$ and denoting $\Omega\tau = \beta$ we obtain the dependance k_2 on τ in a parametric form:

$$\tau(\beta) = \frac{\beta(\cos\beta - R)}{\gamma \sin\beta}, \quad k_2(\beta) = \gamma(\cos\beta - R) + \frac{\beta \sin\beta}{\tau(\beta)}, \tag{3.7}$$

where the parameter β is varied in the interval $(0, \arccos R)$. These boundaries are depicted in Fig. 4 for $R = -0.3$. We see that the EPLCC extends the stability region of the synchronization manifold in the (τ, k) plane. The maximum prediction time can be obtained from Eq. (3.7) in the limit $\beta \to 0$. The necessary condition for stability of the synchronized state is

$$\tau < \tau_H = (1 - R)/\gamma, \tag{3.8}$$

Comparing this with Eq. (2.6) derived for PLCC, we see that the EPLCC extends the prediction horizon by a factor $(1-R)$. Only for negative values of the parameter R this factor is grater then 1. When $R \to -1$ this factor reaches maximal value equal to 2. Thus for coupled spirals, the maximum prediction horizon of the EPLCC exceed two times the maximum prediction horizon of the PLCC. Note that in the case of negative values of R the feedback law (3.2) describes a series with alternating signs. Only such a series advances the stability of anticipating synchronization.

We now consider an application of EPLCC algorithm for chaotic systems in general. We extend Eqs. (1.3) for EPLCC as follows

$$\dot{\mathbf{r}}_1(t) = \mathbf{f}(\mathbf{r}_1(t)) \tag{3.9a}$$
$$\dot{\mathbf{r}}_2(t) = \mathbf{f}(\mathbf{r}_2(t)) + k\mathbf{S}(t), \tag{3.9b}$$

where the perturbation $\mathbf{S}(t)$ is governed by recursive equation

$$\mathbf{S}(t) = \mathbf{K}[\mathbf{r}_1(t) - \mathbf{r}_2(t - \tau) + R\mathbf{S}(t - \tau)] \tag{3.10}$$

and the coupling matrix $\mathbf{K}$ is defined by Eq. (2.11). For $R = 0$ these equations describe the PLCC considered previously. Note that the anticipatory synchronization manifol $\mathbf{r}_2(t) = \mathbf{r}_1(t + \tau)$ is a solution of Eqs. (3.9), (3.10) for any R.

The linear stability of the anticipatory synchronization manifold is determined by variational equations

$$\dot{\mathbf{\Delta}}(t) = \frac{\partial \mathbf{f}}{\partial \mathbf{r}}\Big|_{\mathbf{r}=\mathbf{r}_1(t)} \mathbf{\Delta}(t) - k\mathbf{S}(t - \tau) \tag{3.11a}$$
$$\mathbf{S}(t) = \mathbf{K}[\mathbf{\Delta}(t) + R\mathbf{S}(t - \tau)], \tag{3.11b}$$

where $\mathbf{\Delta}(t) = \mathbf{r}_1(t) - \mathbf{r}_2(t - \tau)$ is a transversal deviation from the synchronization manifold. The growth rates of this deviation define the transversal Lyapunov exponents. A necessary condition for the synchronized regime to be stable is that the maximum transversal Lyapunov exponent $\lambda_\perp$ is negative.

The performance of EPLCC is demonstrated for the Rössler system in Fig. 3 (c) and 6. In Fig. 6 we plot the dependence of $\lambda_\perp$ on the delay time τ. This characteristic is obtained by numerical integration of the variational equations (3.11) together with Eq. (3.9a). The transversal Lyapunov exponent has a minimum at the delay

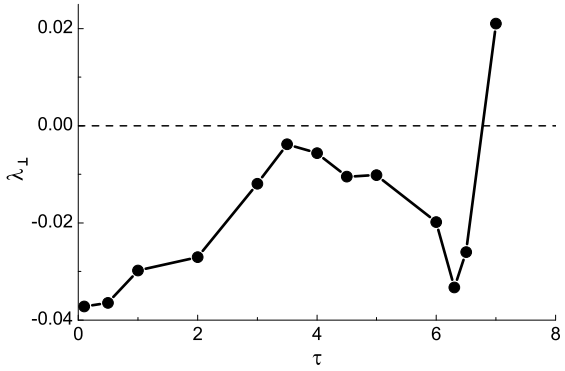

Figure 6. The maximum transversal Lyapunov exponent $\lambda_\perp$ as a function of the prediction time τ for the Rössler system. The parameters of EPLCC are: $R = -0.46$ and $k = 0.18$.

time $\tau \approx 6.3$ coinciding with the characteristic period of chaotic oscillations $T = 2\pi/\omega$, where ω is the frequency of the relevant saddle-fixed point of the strange attractor. Thus the EPLCC provides an optimal prediction for time intervals close to the characteristic period of the strange attractor. In figure 3 (c) we show the dynamics of the drive (3.9a) and response (3.9b) Rössler systems in the case of EPLCC (3.10) with $R = -0.45$. In comparison to the PLCC [cf. Fig. 3 (b)], the EPLCC prolongs the maximum prediction horizon almost two times.

4. Conclusions

We have considered two algorithms that extend the anticipation horizon of chaos synchronization schemes with a time-delay coupling. The algorithms are referred to as a phase-lag compensating coupling (PLCC) and an extended phase-lag compensating coupling (EPLCC). The PLCC utilizes the topological properties of a typical chaotic attractor originated from a saddle-focus fixed point. The main idea is to design the coupling matrix in such a way that it compensates the phase-lag in the time-delayed feedback term of the slave system. The PLCC extends several times the maximum prediction horizon as compared to the diagonal coupling usually used in the literature. The second, EPLCC algorithm, is even more advantageous. It utilizes information from many previous states of the master and slave systems. The idea of EPLCC comes from delayed feedback control theory, where a similar feedback law has shown its merits. The EPLCC modification exceeds about two times the maximum prediction of the PLCC. The maximum prediction time attained with EPLLC is equal to the characteristic period of chaotic oscillations.

The PLCC and EPLLC algorithms can be used as a strategy for real-time forecasting of chaotic dynamics in many technical applications. They can be implemented by analogue technique and are especially advantageous for forecasting the dynamics of fast chaotic systems. We hope that our findings will stimulate the search for appropriate coupling laws in other problems of anticipating synchronization, e.g., to enhance the predictability of chaotic systems with unknown dynamical models [Ciszak *et al.* (2005)] or excitable systems driven by random forcing [Ciszak *et al.* (2003,2004)].

References

Afraimovich, V. S., Verichev, N. N. & Rabinovich, M. I. 1986 Stochastically synchronized oscillations in dissipative systems. *Izv. Vyssh. Uchebn. Zaved. Radiofiz.* **29**, 1050–1060.

Boccaletti, S., Kurths, J., Osipov, G., Valladares, D. L. & Zhou, C. S. 2002 The synchronization of chaotic systems. *Phys. Rep.* **366**, 1–101.

Calvo, O., Chialvo, D. R., Eguíluz, V. M., Mirasso, C. & Toral, R. 2004 Anticipated synchronization: A metaphorical linear view. *Chaos* **14**, 7 –13.

Ciszak, M., Calvo, O., Masoller, C., R Mirasso, C. & Toral, R. 2003 Anticipating the response of excitable systems driven by random forcing. *Phys. Rev. Lett.* **90**, 204102.

Ciszak, M., Marino, F., Toral, R. & Balle, S. 2004 Dynamical mechanism of anticipating synchronization in excitable systems. *Phys. Rev. Lett.* **93**, 114102.

Ciszak, M., Gutiérrez, M., Cofiño, A. S., Mirasso, C., Toral, R., Pesquera, L. & Ortín, S. 2005 Approach to predictability via anticipated synchronization, *Phys. Rev.* E **72**, 046218.

Corless, R. M., Gonnet, G. H., Hare, D. E. G., Jeffrey, D. J., & Knuth, D. E. 1996 On the Lambert W function. *Advances in Computational Mathematics* **5**, 329.

Fiedler, B., Flunkert, V., Georgi, M., Hövel, P. & Schöll, E. 2007 Refuting the odd-number limitation of time-delayed feedback control. *Phys. Rev. Lett.* **98**, 114101.

Gauthier, D. J., Sukow, D. W., Concannon, H. M. & Socolar, J. E. S. 1994. Stabilizing unstable periodic orbits in a fast diode resonator using continuous time-delay autosinchronization, *Phys. Rev. E*, **50**, 2343–2346.

Kostur, M., Hänggi, P., Talkner, P. & Mateos, J. L. 2005 Anticipated synchronization in coupled inertial ratchets with time-delayed feedback: A numerical study. *Phys. Rev.* E **72**, 036210.

Mainieri, R. & Rehacek, J. 1999 Projective synchronization in three-dimensional chaotic systems. *Phys. Rev. Lett.* **82**, 3042–3045.

Masoller, C. 2001 Anticipation in the synchronization of chaotic semiconductor lasers with optical feedback. *Phys. Rev. Lett.* **86**, 2782–2785.

Mendoza, C., Boccaletti, S. & Politi, A. 2004 Convective instabilities of synchronization manifolds in spatially extended systems. *Phys. Rev.* E **69**, 047202.

Pecora, L. M. & Carroll, T. L. 1990, Synchronization in chaotic systems. *Phys. Rev. Lett.* **64**, 821–824.

Pikovsky, A., Rosemblum, M. & Kurths, J. 2001 *Synchronization: A universal concept in nonlinear sciences*. Cambridge: Cambridge University Press.

Pyragas, K. 1992 Continuous control of chaos by self-controlling feedback. *Phys. Lett.* A **170**, 421–428.

Pyragas, K. 1995 Control of chaos via extended delay feedback. *Phys. Lett.* A **206**, 323–330.

Pyragas, K. 1996 Weak and strong synchronization of chaos. *Phys. Rev.* E **54**, R4508–4512.

Pyragas, K. 1998 Synchronization of coupled time-delay systems: analytical estimations. *Phys. Rev.* E **58**, 3067–3071.

Pyragas, K. 2006 Delayed feedback control of chaos. *Phil. Trans. R. Soc* A **364**, 2309-2334.

Pyragas, K. & Pyragienė, T. 2008 Coupling design for a long-term anticipating synchronization of chaos. *Phys. Rev.* E **78**, 046217.

Rosenblum, M. G., Pikovsky, A. S. & Kurths, J. 1996 Phase synchronization of chaotic oscillators. *Phys. Rev. Lett.* **76**, 1804–1807.

Rosenblum, M. G., Pikovsky, A. S. & Kurths, J. 1997 From phase to lag synchronization in coupled chaotic oscillators. *Phys. Rev. Lett.* **78**, 4193–4196.

Rössler, O. E. 1976 An equation for continuous chaos. *Phys. Lett.* A **57**, 397–398.

Rulkov, N. F., Sushchik, M. M., Tsimring, L. S. & Abarbanel, H. D. I. 1995 Generalized synchronization of chaos in directionally coupled chaotic systems. *Phys. Rev.* E **51**, 980–994.

Sivaprakasam, S., Shahverdiev, E. M., Spencer, P. S. & Shore, K. A. 2001 Experimental demonstration of anticipating synchronization in chaotic semiconductor lasers with optical feedback. *Phys. Rev. Lett.* **87**, 154101.

Tang, S. & Liu, J. M. 2003 Experimental verification of anticipated and retarded synchronization in chaotic semiconductor lasers. *Phys. Rev. Lett.* **90**, 194101.

Voss, H. U. 2000 Anticipating chaotic synchronization. *Phys. Rev.* E **61**, 5115 – 5119.

Voss, H. U. 2001 Dynamic long-term anticipation of chaotic states. *Phys. Rev. Lett.* **87**, 014102.

Voss, H. U. 2002 Real-time anticipating of chaotic states of an electronic circuit. *Int. J. Bifurc. Chaos Appl. Sci. Eng.* **12**, 1619–1625.